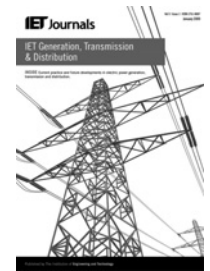


Published in IET Generation, Transmission & Distribution
 Received on 10th May 2013
 Revised on 28th October 2013
 Accepted on 17th January 2014
 doi: 10.1049/iet-gtd.2013.0323



ISSN 1751-8687

End user voltage regulation to ease urban low-voltage distribution congestion

Gordon Connor, Catherine E. Jones, Stephen J. Finney

Department of Electronic and Electrical Engineering, University of Strathclyde, Royal College Building, 204 George Street, Glasgow, G1 1XW, UK

E-mail: gordon.connor@strath.ac.uk

Abstract: Owing to the increasing demand in the urban areas for new technologies such as heat pumps and electric vehicles (EVs), greater power capacity in low voltage (LV) distribution networks is becoming increasingly important. This study will investigate how to improve the power capacity through the implementation of point of use voltage regulation (PUVR). PUVR relies on a power electronics converter at each end-user. Most LV network cabling has a voltage limit of 1 kV, PUVR exploits this voltage rating to increase the network capacity. This study will describe and discuss the results from a viability study using data from a utility company, which shows that the capacity in the LV network could be increased by an additional 500 kVA. However, it was also found that PUVR using present off-the-shelf converters is not as cost-effective as replacing the LV network cables. Two power electronics topologies have been investigated in the simulation studies to date: the AC chopper circuit and the back-to-back inverter circuit. These two topologies were compared and the AC chopper was found to be a cheaper, more efficient topology. Therefore the AC chopper is more suitable for this application and may increase the viability of the PUVR.

1 Introduction

1.1 Need for point of use voltage regulation (PUVR)

In order for the UK to meet the 2020 and 2050 greenhouse gas emissions targets set by the European Union, immediate changes are required across all energy sectors [1]. Therefore it is expected that over the next 30 years ‘cleaner’ emerging technologies such as heat pumps [2] and electric vehicles (EVs) will be implemented in order to meet these targets. In addition, the price of fossil fuels is expected to rise significantly, possibly by up to as much as 30% in one year [3]. The increasing costs of fossil fuels and of new vehicles are likely to force higher population densities in urban areas, thereby reducing distance of travel to the work place. Therefore it is prudent to assume a large increase in load on urban distribution systems [4] in the future.

If the existing urban low-voltage distribution infrastructure is left unchanged, it is unlikely to be ready for this predicted increase in demand in urban areas, which is expected to be in the order of 1–2 GW in magnitude [4]. The aim of this paper is to show that end user voltage regulation is a potential solution to this problem. The concept of PUVR is to set the line-to-line voltage in the three-phase distribution cabling to be higher than the standard 415 V. At present, the insulation limit of the wiring allows a maximum of 1 kV [5]. Therefore it is clear that the distribution cabling is

underutilised, but in order to make the power usable when it reaches the customer it must be transformed down to 230 V phase.

1.2 Advantages of using PUVR

1.2.1 Voltage rise: The voltage drop as current travels through a conductor is dependent on the impedance of the conductor [6]. Considering a street of houses in an urban distribution system, to ensure each house receives 230 V, including the housing at the end of the conductor, it is acceptable for the voltage to fluctuate within the limits of 230 V + 10–6% [7].

PUVR can be used to overcome this problem of fluctuating voltage, resulting in each house on the distribution network receiving exactly 230 V AC. This paper will demonstrate how this level of control can be achieved using power electronics whereas conventional distribution networks use transformers to control voltage amplitude.

1.2.2 Distributed generation: The integration of distributed generation on the distribution grid close to the point of use reduces transmission losses and helps to meet local power demand [8]. This is particularly useful during times of peak demand. However, during periods of off-peak demand where there is significant reduction in the local load, local distributed generation will contribute to the voltage rise. This can lead to the voltage rise exceeding

acceptable standards [9]. In addition, the reverse current limit of the local distribution transformer may be exceeded [10]. As previously stated an urban distribution network which uses PUVR is able to negate the voltage rise problem. The main disadvantage of using PUVR is that replacement transformers would be required because of higher voltage ratings, however, a replacement transformer may be necessary in any case to address this issue.

1.2.3 Power electronics against transformers: The introduction of PUVR would reduce the reliance of the distribution network on transformers to regulate voltage levels. The use of power electronics is advantageous over transformers for this purpose as the implementation of the modulated switching control around power electronics is easier to implement than control of a tap changing transformer.

Modern power electronics are as efficient as traditional transformers in addition to having a smaller form factor [11, 12]. Power electronics are also more cost efficient. It is expected that a power electronic converter would cost half as much as an equivalent transformer [13–16].

1.2.4 Electric vehicles: Personal transport accounts for 13% of the UKs emissions. One possible way of reducing this is the introduction of EVs [17]. Widespread charging of EVs will increase the electricity demand on the low-voltage infrastructure from 4 to 19 kW at each end-user [18]. PUVR would increase the capacity available for this extra load and would also assist in the charging speed of the EV [19, 20].

A similar concept to PUVR has been explored in Sweden in preparation for the increased loading cause by EVs [19]. It found that raising the voltage to 1 kV on existing cables can be used as a method to reinforce the low-voltage network. It also states that this method can be more cost effective than replacing the existing infrastructure with higher capacity conductors. The example study found the cost of replacing the conductors was 56% greater than creating a 1 kV network with transforming equipment.

1.3 Paper outline

This paper will first investigate the need for PUVR by considering the congestion limits of the present urban distribution system and consider how the capacity of an urban distribution network could be increased by implementation of PUVR. Secondly two options for implementing a PUVR system will be described: a back-to-back converter topology and an AC chopper topology. These two possible solutions will be compared considering losses, power quality, complexity, control and protection.

2 Congestion studies on the present low-voltage urban distribution network

2.1 Low-voltage distribution cable limitations

The cables used in low-voltage distribution have a maximum voltage limit, based on the insulation, of 1 kV [5]. The current limit varies with the type of conductor, but typical ratings are 155–415 A (taken from industry average conductor size). The higher the current and thermal rating of the cable, the higher the cost of the cable.

Typical industry cost for a length of copper underground cable, of area 16 mm², is 0.71 £/m (costing information received from industry partners) and has a current limit of 111 A while a 35 mm² copper cable costs 1.29 £/m and has a current limit of 178 A. Therefore there is a clear trade-off between line cost and its thermal (and hence capacity) limitations. In the simulation studies carried out, the cables were modelled using typical parameters of cables used in urban distribution networks.

2.2 Limits of the present urban distribution system

A section of the low-voltage distribution system was modelled using Power World simulator in order to study the current limits. This model was based on real data for a representative section of the UK distribution network: it was created from a diagram received from industry partners which specified the length and type of each cable. A separate document which specified resistance and reactance per length and cable type was then used to calculate the total resistance and reactance for each line. The characteristics of each cable could then be entered into Power World simulator; the data for each cable is presented in Appendix 1. The model enabled the study of thermal losses in the distribution system because of current levels, hence enabling the current limits of the low-voltage distribution system to be studied. In these simulations, it is assumed that each end user is a three bedroom house consuming 3500 kWh/year. Since demand is not easy to predict and has a random element it was expected that the demand pattern would be short spikes in demand occurring randomly over long periods of smaller base demand. The present low voltage cabling was designed for this demand pattern (see Fig. 1a). When all of the random demands are amalgamated the overall demand of an area will generally be consistent. This random element is not possible to simulate in Power World simulator and as a result all spike and base demands were averaged. This means that results from the main feeders will be the most accurate. The maximum average demand for each house was taken to be a constant demand of 1 kW per household, this corresponds to early evening in winter in the UK [21].

Fig. 1 shows the results of this study. By inspection of Fig. 1a it can be seen that the main feeder is at 65% of its thermal capacity. This simulation result indicates that, without PUVR, a further 174 A could be drawn from the distribution network before the thermal limit of the main feeder reached 100% capacity. From the used assumptions this is the equivalent of 124 more houses.

If EVs or heat pump boilers were introduced to the present system it would more than double average household load [2, 18, 22]. The effect of doubling the average load at each household to 2 kW is shown in Fig. 1b. This indicates that the capacity of the network cannot be increased by increasing current levels because of the thermal limit of the network. Therefore to increase the capacity of the network, increasing the voltage level of the system must be considered. A realistic way to achieve this would be using PUVR.

2.3 Effect of implementing voltage regulation

The effect of increasing the voltage on the distribution network is shown in Figs. 1c and d. Fig. 1c has a network voltage level of 600 V, while in Fig. 1d the voltage level is increased further to 1 kV.

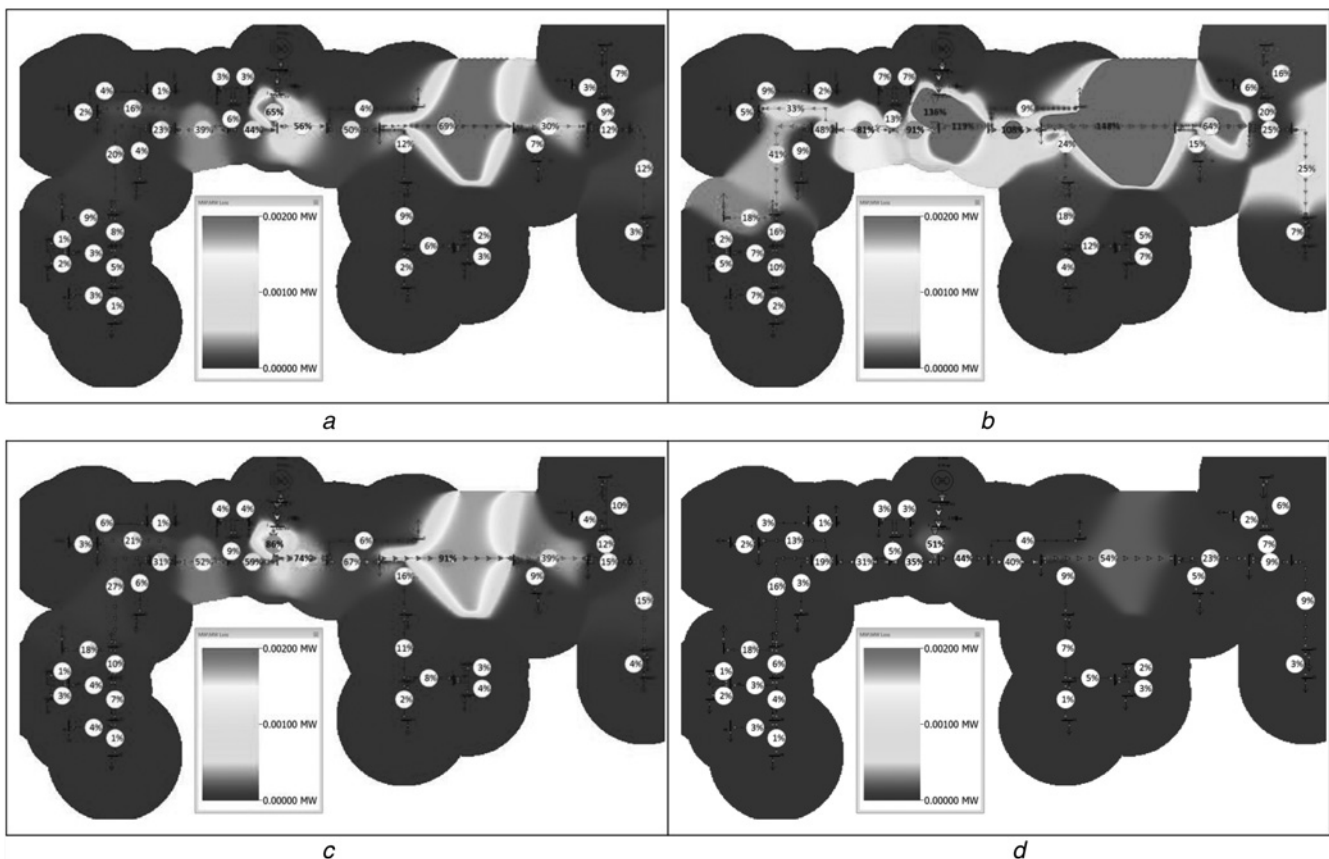


Fig. 1 Heat maps of power loss: darkest areas show 0 W loss, palest show 2 kW loss

- a* Average loading
b Double average loading conditions
c Double average loading at 600 V
d Double average loading at 1 kV

Although setting the network voltage at 1 kV would provide the most effective voltage regulation, it is only being shown here as a comparison. It is not a viable option because of the cable insulation limit of 1 kV. In reality the cable insulation limit will be below 1 kV because of factors such as tolerances, degradation and bends/twists in the cabling [23].

From Fig. 1*c*, it can be observed that the main feeder is now 86% utilised under double average load. This is a decrease from 136% in the results presented in Fig. 1*b*. This means that no cables need to be replaced and a further 24 houses could be placed on the system. This is an increase of 200 kVA in available capacity compared to the present system (Fig. 1*a*). Fig. 1*d* shows a further decrease from 136 to 51% utilisation, 84 new houses could be placed on this system. This is an increase of 500 kVA in available capacity compared to the present system (Fig. 1*a*).

Therefore these studies indicate that PUVR will significantly increase the load capacity of urban distribution networks.

2.4 Consideration of losses in a point of use regulation system

In Section 2.3, PUVR has been shown to be an effective means of increasing the capacity of an urban distribution network. However, the losses attributed to end-user conversion in a PUVR system must be considered. The two main sources of loss are cable losses and converter losses.

2.4.1 Cable loss: From the heat maps in Fig. 1, it is clear that PUVR lowers the thermal losses present in the cabling because of the lower current levels in the network. Table 1 summarises the different thermal losses for the urban

Table 1 Summarises the different thermal losses for the urban distribution network

	415 V average load (Fig. 1 <i>a</i>)	415 V double average load (Fig. 1 <i>b</i>)	600 V double average load (Fig. 1 <i>c</i>)	1 kV double average load (Fig. 1 <i>d</i>)
<i>(a) Cable loss at average load and double average load at each voltage level</i>				
cable loss, %	3.1	6.74	1.26	0.16
<i>(b) Cumulative loss (cable and conversion) with the best and worst case conversion loss for each voltage level</i>				
cable loss plus converter loss, %	600 V (+2% conversion) 3.26	1 kV (+2% conversion) 2.16	600 V (+8% conversion) 9.26	1 kV (+8% conversion) 8.16

distribution network considered in Fig. 1 operating at different voltage levels.

The present urban distribution network, drawing the maximum average from all loads simultaneously, loses 3.1% of its transmitted power as heat in the cabling. At the estimated future maximum average load, 6.74% of the power transmitted is lost. Transmission of power at 600 V decreases this loss at maximum load to 1.26% and transmission at 1 kV furthers this decrease to 0.16%. These losses were calculated by using the following equation

$$\%_{\text{cableloss}} = \frac{\sum S_{\text{cableloss}}}{S_{\text{in}}} \times 100 \quad (1)$$

2.4.2 Converter loss: When using PUVR, the voltage level must be stepped down at the end-user. In the case of the urban network, this would take place at each house connected to the distribution network.

This voltage conversion will not be 100% efficient, and therefore extra losses will be introduced to the network. Existing power electronic inverters on the market have a maximum efficiency of 98% [24].

The best and worst case scenarios are shown in Table 1. The best case considered was an efficient single conversion process of 2%, with one AC to AC converter. For example, a single phase AC chopper or matrix converter, as shown in Fig. 2a [25]. The worst case considered was an inefficient conversion of 4% using a back-to-back inverter topology [26], as shown in Fig. 4a, this requires two conversions and would, therefore give an 8% conversion loss.

2.5 Cost benefit

The approximate cost of implementing PUVR is shown in Table 2. The costs of transformer and cable replacement including excavation and reformation were taken from the Scottish and Southern Energy (SSE) 2012 Statements, Methodology, Charges and Connection document [27].

Using this document and the diagram gained from industry partners which specify cable length and type (see Section 2.2) an estimation of the cost of replacing the distribution cables was made. The cost of the converters was estimated using the cost of present off-the-shelf converter units [28, 29]. A transformer replacement was considered for the cable replacement method as it is possible that the voltage rise because of the distributed generation issue would give cause to replace this transformer (see Section 1.2.2); a replacement was not deemed necessary for this study.

It was found that, at present, the PUVR method has a greater cost and that a 23 kW converter would need to cost between £460 and £2100 (worst case and best case, respectively) to be equivalent to replacing the cables. However, the costing for these converters was for individual units and it is expected that the price would reduce significantly if ordered in bulk (in this case 220 units). It is also expected that when PUVR is taken into consideration semi-conductor costs would be lower than they are at present as the cost of semi-conductor devices decreases over time [30].

2.6 Summary

The studies carried out have strongly indicated that PUVR would be effective in easing congestion of low-voltage urban distribution systems by increasing capacity of the

network without exceeding thermal/current limits of the cables. A potential disadvantage of implementing PUVR using power electronic converters is that conversion losses are introduced to the system. However, the studies and Tables 1a and b have shown that this additional loss is compensated for by the lower losses in the conductors because of the lower current levels. It was found that PUVR is not as cost-effective as replacing the LV distribution cables. It is expected, however, that future decreases in semi-conductor costs and bulk orders will bring the cost to a comparable level with the cable replacement method.

3 Proposed technology options for PUVR

If the distribution network voltage is raised above 415 V line to increase network capacity, then this voltage must be regulated at each end user on the network to an acceptable level, typically 230 V phase. This paper proposes two different power electronic circuits to carry out the voltage regulation: the AC chopper and the back-to-back inverter.

3.1 AC chopper for PUVR

Fig. 2a shows the initial design of the AC chopper, which is the single phase form of the matrix converter [25], the circuit V_{in} is 346 V AC (from 600 V line to single phase) which is pulse-width modulated at 10 kHz by the IGBT switching arrangement S1–S4.

Activation of switches S1 and S2 will connect the load to the source voltage, while activation of S4 and S3 will apply zero voltages to the load. Modulation of these states allows the load voltages to be controlled as shown in Fig. 2b. The resulting output is then filtered by a low-pass filter shown in Fig. 2a as an inductance 'L'. The final output is a controlled 230 V AC waveform at 50 Hz shown in Fig. 2c.

3.1.1 Filter design: The AC chopper introduced harmonics to the input current, output voltage and output current in the form of multiples of the switching frequency (10 kHz) each at 50% total harmonic distortion (THD). To reduce this distortion, the output voltage and current must be filtered in order to meet acceptable power quality standards [26]. Therefore an inductive first-order filter with a cut-off frequency of 75 Hz was designed.

As a filter with this cut-off frequency is able to filter the high frequency harmonics of the switching and additionally filter lower frequency harmonics because of non-linear loading, which typically are at odd multiples of the fundamental [31]. The open-loop transfer function for the first-order filter is given as follows

$$\frac{V_{\text{out}}}{V_{\text{in}}} = \frac{R}{R + sL} \quad (2)$$

$$\omega_n = \frac{R}{L} \quad (3)$$

The cut-off frequency of the filter was chosen to be 75 Hz as this is between the fundamental and second harmonic frequencies ensuring the third harmonic is filtered. This is represented in angular frequency by $\omega_n = 471 \text{ rads}^{-1}$ and using an average household load of $R = 53 \Omega$ (taken from the earlier three bedroom household consumption average of 3500 kWh/year, Section 2.2) using (3) the optimum value for L was calculated to be 112.5 mH.

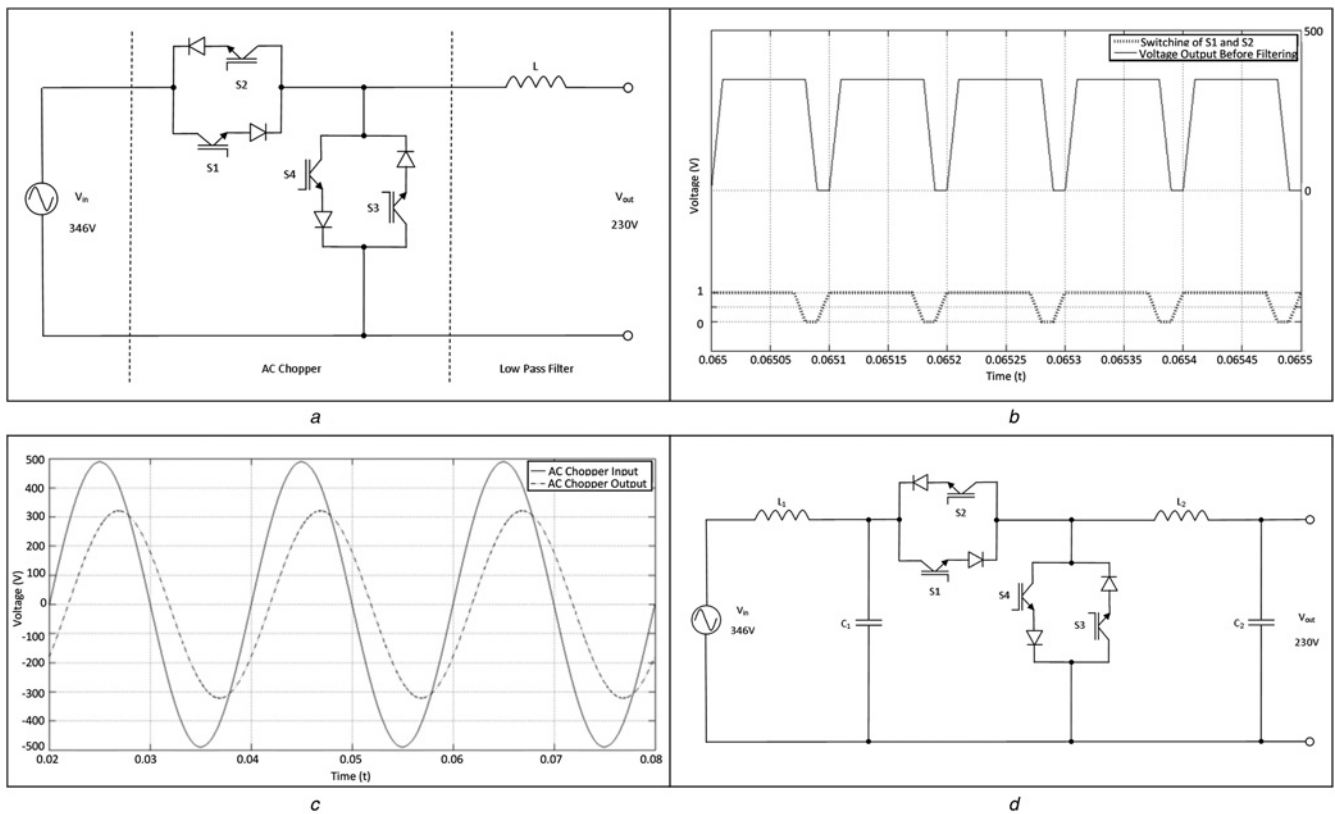


Fig. 2 Single phase AC chopper or matrix converter

- a Initial AC chopper circuit design
- b Switching pattern of forward conducting AC chopper
- c AC chopper input and output at steady state. Switching at 10 kHz with inductive filter of value 112.5 mH
- d Final AC chopper circuit design

3.1.2 AC chopper results: Fig. 2c demonstrates the steady-state operation of the AC chopper it is clear that the circuit successfully lowers a voltage of 346 to 230 V. A phase shift of 32° between the waveforms can also be observed, this is, because of the inductance in the low-pass

filter (see Fig. 2a). This phase shift is not detrimental to the operation of the circuit.

To improve the design of the AC chopper, firstly, the filter was redesigned as a second-order filter, which included a capacitor, therefore increasing the response time of the filter

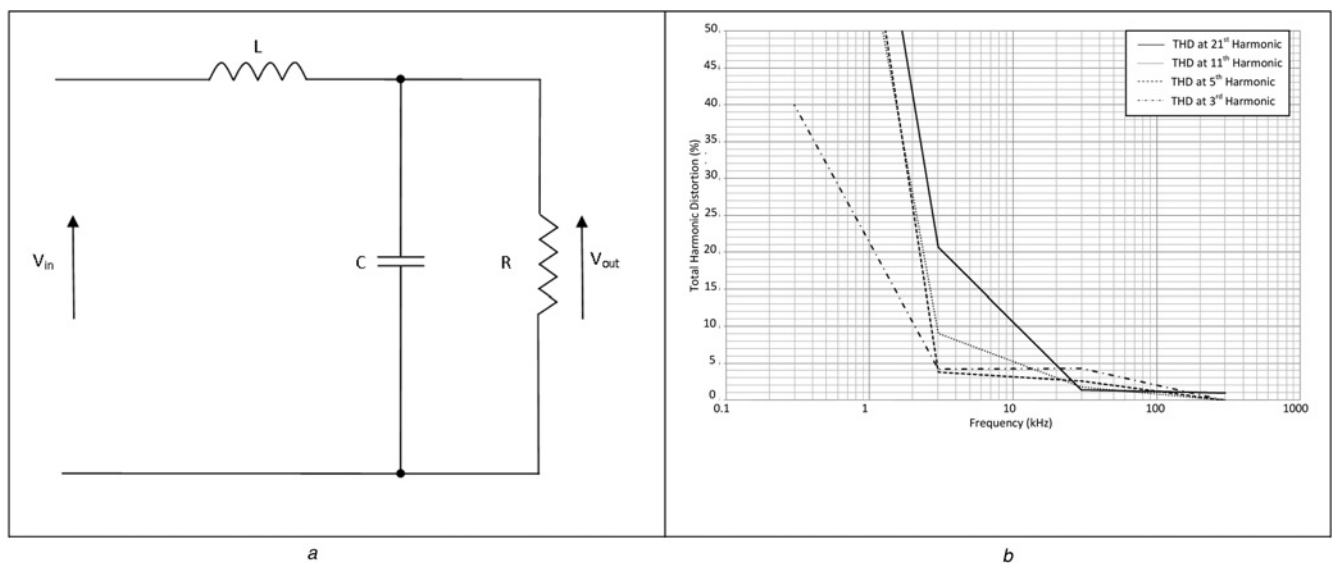


Fig. 3 Filter designed to filter out the 21st harmonic

- a Second-order filter
- b Distortion of input current against switching frequency

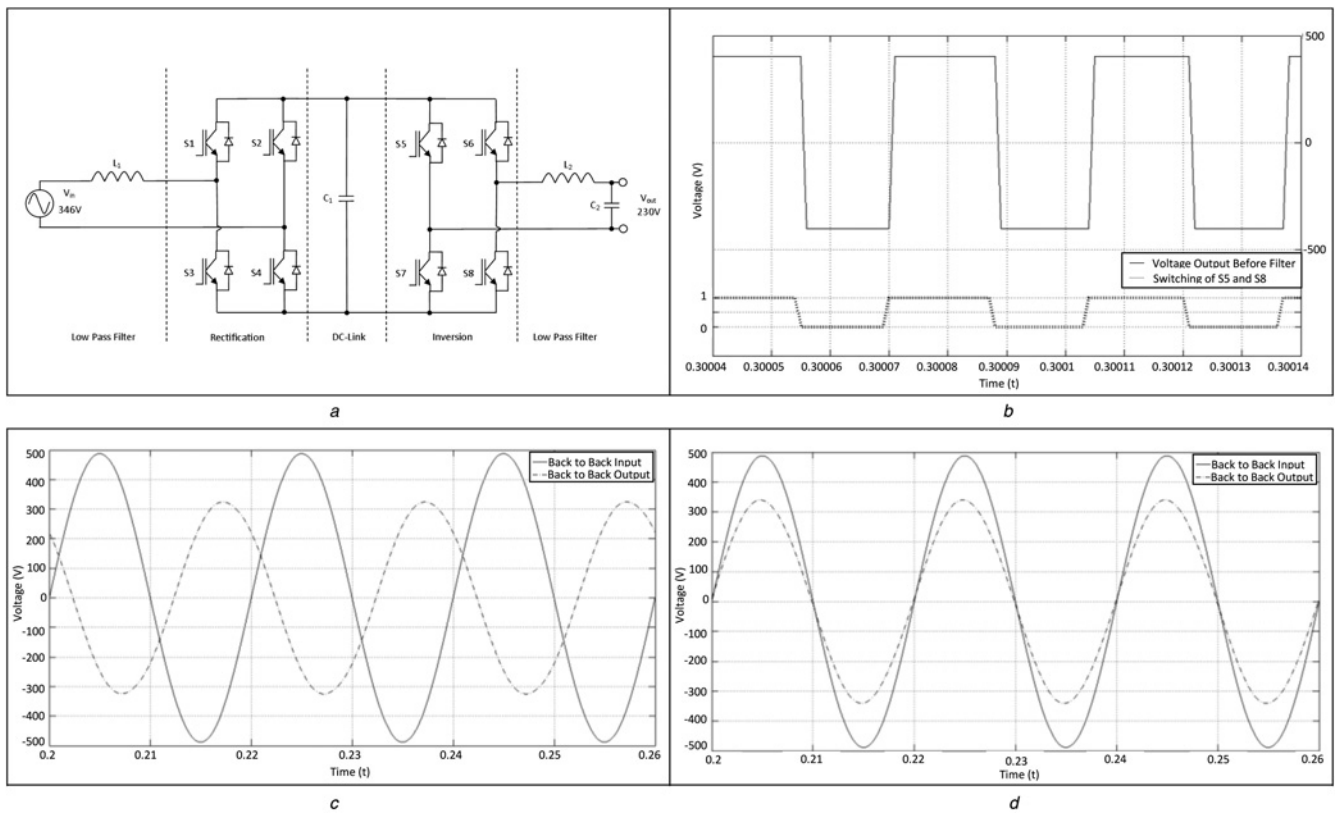


Fig. 4 Circuit topology for the back-to-back inverter

- a Circuit diagram of back-to-back inverter
- b Switching pattern of the inversion stage
- c Back-to-back inverter initial input and output
- d Back-to-back inverter steady-state phase compensated

and decreasing the magnitude of any passed higher frequencies (see Section 3.2.3). Secondly, the switching frequency was adjusted to 33 kHz minimising voltage harmonics in the output (see Section 3.2.4). Thirdly an input filter was introduced to the AC chopper, to minimise current harmonics at the input caused by non-linear loading, see Fig. 2d.

3.1.3 Second-order low-pass filter design: The transfer function of a second-order low-pass filter (Fig. 3a) is given in (4). In order to tune this filter to give the desired response, the transfer function in (4) was manipulated to have the form of a standard second-order transfer function as shown in (5). By comparison of (4) with (5) the values for the inductance and capacitance for a given cut-off frequency can be calculated, using (6) and (7)

$$\frac{V_{out}}{V_{in}} = \frac{((R/sC)/(R+(1/sC)))}{(R/sC)/(R+(1/sC))+sL} \quad (4)$$

$$\frac{V_{out}}{V_{in}} = \frac{\omega_n^2}{s^2 + 2\omega_n\xi s + \omega_n^2} \quad (5)$$

$$\omega_n = \sqrt{\frac{1}{LC}} \quad (6)$$

$$2\omega_n\xi = \frac{1}{RC} \quad (7)$$

Since $R = 53 \Omega$, $\omega_n = 471 \text{ rad s}^{-1}$ and $\xi = 1$ using (6) and (7) the optimum values for L and C were calculated to be: $L = 225 \text{ mH}$ and $C = 20 \mu\text{F}$.

It was found that the new filter design is an improvement as, post cut-off frequency, the first-order filter has a slope of 19.2 dB/decade and the second-order filter has a slope of 37.3 dB/decade.

3.1.4 Switching frequency against harmonic distortion: In order to optimise the size of the filter an

Table 2 Cost benefit results

Proposed method	Cost of transformer replacement, £		Cost of cable replacement, £		Cost of converters, £		Total cost, £	
	Min	Max	Min	Max	Min	Max	Min	Max
PUVR method	13 800	69 200	N/A	N/A	621 500	1 335 800	635 300	1 405 000
cable replacement method	N/A	N/A	169 700	476 600	N/A	N/A	169 700	476 600

analysis of harmonic distortion and switching frequency was carried out. The focus was to minimise harmonic content caused by the introduction of the AC chopper while also trying to minimise filter size. A higher switching frequency will increase the frequency of the harmonics, therefore the size of the filter can decrease [31]. The filter was redesigned to filter the 3rd, 5th, 11th and 21st harmonics of the fundamental. These new filter values were tested against differing switching frequencies the result of this is shown in Fig. 3b. The British standards (Energy Networks Association – G5/4) limit for THD is 5% [31].

From Fig. 3, a filter designed to filter out the 21st harmonic of the fundamental combined with a switching frequency of 33 kHz was chosen as optimal. From the results shown in Fig. 3 this allows the use of a small filter without the distortion becoming greater than 5%. The new value of L_1/L_2 is 2 mH and the new value of C_1/C_2 is 0.6 μ F.

The final circuit arrangement for the AC chopper is shown in Fig. 2d; note that an input filter of equal magnitude has been added. This filter limits the harmonics present in the input current. For further information on harmonics see Section 4.2.

3.1.5 Back-to-back inverter: Fig. 4a shows the circuit topology for the back-to-back inverter. As with the improved chopper, it is proposed that the switching frequency is 33 kHz, with an input voltage level of 346 V single phase AC. The back-to-back inverter consists of an active rectifier and inverter.

The inversion process is shown in Fig. 4b, it can be observed that the output contains switching frequency components therefore a filter is required to smooth the signal, shown in Fig. 4a as inductance L_2 and capacitance C_2 .

3.1.6 Capacitor sizing and design of input and output filters: The size of the DC-link capacitor has an effect on voltage ripple on the DC section of the topology. Large values of ripple will have an adverse effect on circuitry lifetime [32], therefore minimising this value is prudent. However, increases in DC-link capacitor size increase the time taken to reach steady state [33]. Equation (8) is used to calculate the voltage ripple [26, 33]

$$V_{\text{ripple}} = \frac{V_{\text{peak}}}{2 \times R_{\text{load}} \times C_1} \times T \quad (8)$$

where T is the switching period (20 ms), V_{peak} is the highest voltage point (600 V), R_{load} is the load resistance (53 Ω) and V_{ripple} is the ripple in the DC voltage. It is known that (8) becomes increasingly inaccurate for a voltage ripple higher than 10% [34]. Hence minimum DC-link capacitance required for a 10% ripple was calculated to be 1.88 mF. The sizing and importance of the input inductance is described in Section 4.2.

For the output filter, the same process of filter choice was used as described in Section 3.2.4. Therefore the values

used in the back-to-back inverter output filter were $L_2=2$ mH and $C_2=0.6$ μ F at a switching frequency of 33 kHz.

3.1.7 Back-to-back inverter results: Fig. 4c illustrates the input and output voltage from the back-to-back inverter. By inspection of Fig. 4c it can be seen that the output voltage is shifted by 171° leading. Unlike the AC chopper, which pulse-width-modulates the input voltage and draws a chopped version of the output current. The back-to-back inverter deconstructs the voltage into DC.

The back-to-back inverter can then synthesise an AC voltage of any phase, magnitude and frequency. Therefore the control of the input and output stage are decoupled. The phase shift can be compensated for in the control, this is shown in Fig. 4d.

4 Comparison of the AC chopper and back-to-back inverter for PUVR

The two topologies presented in the previous section have been tested in simulation and results for their performance in several areas compared. They were compared in the following areas:

- Losses
- Power quality
- Complexity
- Control
- Transient behaviour
- Protection

4.1 Losses

The conduction loss for the AC chopper and back-to-back inverter was calculated and is shown in Table 3. These results were calculated using the data in the device datasheets [35, 36] and the loss calculation methods used in [26, 37, 38].

The switching losses for both of the topologies were calculated, using a switching frequency of 33 kHz. The energy loss for each time the devices switched was taken from the device datasheet. The results of these calculations are shown in Table 3. In order to validate the calculations the back-to-back inverter and AC chopper were both modelled in PLECS. The models calculated the conduction and switching losses; with a thermal profile for each device created from information in the device datasheets [35, 36]. These results indicate that the back-to-back inverter generates approximately 6–7% more total loss than the ac chopper.

4.2 Power quality

Equation (9) [39] is used to describe the transmission of real power between two sources linked by a series inductance. Examining Fig. 4a it can be said that because of the

Table 3 Summary table of device losses: switching and conduction

Loss	$P_{\text{conduction}}, \text{W}$		$P_{\text{switching}}, \text{W}$		Total, W		Total, %	
	Calculation	PLECS	Calculation	PLECS	Calculation	PLECS	Calculation	PLECS
back-to-back inverter, per arm	2.01	2.7	10.3	9.3	98.5	96	9.8	9.6
AC chopper, per arm	2.2	3.2	4.5	5.9	27	36.4	2.7	3.6

Table 4 Summary table of THD on both topologies

Device and configuration	V_{in} THD, %	I_{in} THD, %	V_{out} THD, %	I_{out} THD, %
AC chopper (linear load)	0	0.81	0.44	0.44
AC chopper (non-linear load)	0	58.9	16.1	58.8
back-to-back inverter (linear load)	0	0.29	0.17	0.17
back-to-back inverter (non-linear load)	0	3.05	3.45	69.9

inductive element between the grid and the rectifier (9) is true for the back-to-back inverter

$$P = \frac{V_1 \times V_2}{X} \times \sin(\delta_1 - \delta_2) \quad (9)$$

where V_1 is the voltage of the primary source at angle δ_1 (346 V_{rms}), V_2 is the voltage of the secondary source at angle δ_2 (425 V_{rms}) and X is the reactance of the inductance L (0.02 H) multiplied by the angular frequency (100π). Therefore from (9), we can state that the real power bandwidth between the grid and the back-to-back inverter rectification stage is 0–23 kW dependant on the phase difference between the two.

4.2.1 Total harmonic distortion: Two Matlab models using idealised lossless devices were implemented to study the effect of non-linear loads on system power quality. Table 4 is a summary of the effects of THD on both topologies. First the THD of both topologies was found with a standard linear load of 53 Ω . Subsequently both topologies were tested with non-linear loads added in parallel with the linear load. The five non-linear loads were a TV, laptop, games console and desktop PC with display. These were modelled as a diode bridge rectifier attached to a resistance with a parallel capacitance; the value of resistance was calculated using the power draw of these loads. The power draw data was gained from examining the power electronic transformers of these loads (see Appendix 2).

It was found that adding a switching device would introduce a small amount of THD at each end-user, if PUVr were implemented this would have to consist with industry standards.

It can be observed that the back-to-back inverter has a much lower level of THD at the input when subjected to large non-linear loads. In reality, the THD of these non-linear loads is much less, as conducted harmonic emissions are restricted by standards. However, for the purposes of this study a worst case scenario has been assumed. The back-to-back inverter topology shows a decrease in harmonic content from the output to the input.

Table 6 Power quality results from varying the load

Power draw, W	Device	P_{in} , W	Q_{in} , VAR	P_{out} , W	Q_{out} , VAR	V_{in} THD, %	I_{in} THD, %	V_{out} THD, %	I_{out} THD, %
100	AC chopper	100	-32.2	100	0	0	3.98	0.48	0.48
	back-to-back inverter	100	-0.2	100	0	0	3.12	1.83	1.83
1000	AC chopper	1000	15	1000	0	0	0.81	0.44	0.44
	back-to-back inverter	997	0	997	0	0	0.29	0.17	0.17
10 000	AC chopper	10 000	1700	10 000	0	0	0.77	0.42	0.42
	back-to-back inverter	10 000	-1	9973	0	0	2.03	0.11	0.11
20 000	AC chopper	20 000	7100	20 000	0	0	1.15	0.61	0.61
	back-to-back inverter	20 010	2480	19 960	0	0	4.98	0.06	0.06

Table 5 Summary table of power with and without reactive load

Device and configuration	P_{in} , W	Q_{in} , VAR	P_{out} , W	Q_{out} , VAR
AC chopper (R)	1,000	15	1,000	0
AC chopper (R + L)	990	86	990	101
back-to-back inverter (R)	997	0	997	0
back-to-back inverter (R + L)	988	0	988	101

For the back-to-back inverter (see Fig. 4a) the initial rectifying stage can be controlled in order to gain the necessary power for the rest of the circuit.

This decouples the source and the load; with the DC-link capacitor acting as a buffer. Therefore it is reasonable to expect that in terms of power quality the back-to-back inverter will perform better as the AC chopper has no similar function, see Fig. 2d.

4.2.2 Non-unity power factor loading: The effect of reactive loading on the idealised models of both topologies can be shown in Table 5. Each topology was examined with a resistive load (R) of 53 Ω (see Section 3.1.1) and then subsequently tested with the same resistive load in series with an inductive load (L) of 17.2 mH. The value of reactive load was chosen to give a power factor in the region of 0.9.

It was observed that under reactive loading the AC chopper demands the extra 100 VAR required for the load directly from the source. In contrast the back-to-back inverter topology requires no additional reactive power from the source. Based on these observations, the back-to-back inverter is the superior topology with regard to power quality as it has been shown to reject load harmonics and load reactive power draw.

4.2.3 Loading extremes: Although an average load of 1 kW has been assumed it is far more likely that load will erratically vary over the course of the day. The maximum power that can be drawn in a UK household is 23 kW through a 100 A fuse. The results of changing the power drawn is shown in Table 6.

It was found that the back-to-back inverter delivers better power quality at different extremes of loading. In experiencing greater loads the AC chopper required more reactive power for its passive filters, which caused a non-unity power factor. Table 6 shows that conducted emissions from the converter can be controlled, via the use of filters, to be within the boundaries issued in G5/4 (<5% THD [31]).

Table 7 AC chopper and back-to-back inverter primary components cost comparison

Device	1 Bridge arm, £	1 module, £	Cost to convert an urban area, £
AC chopper	9.60	520	111 800
back-to-back inverter	5.76	1070	228 300

Radiated electromagnetic interference (EMI) is a problem associated with the use of power electronics; however at these power levels well established rules for enclosures, connection layout and semi-conductor gate drive devices can be used to ensure EMI is minimised [31].

4.3 Complexity and cost

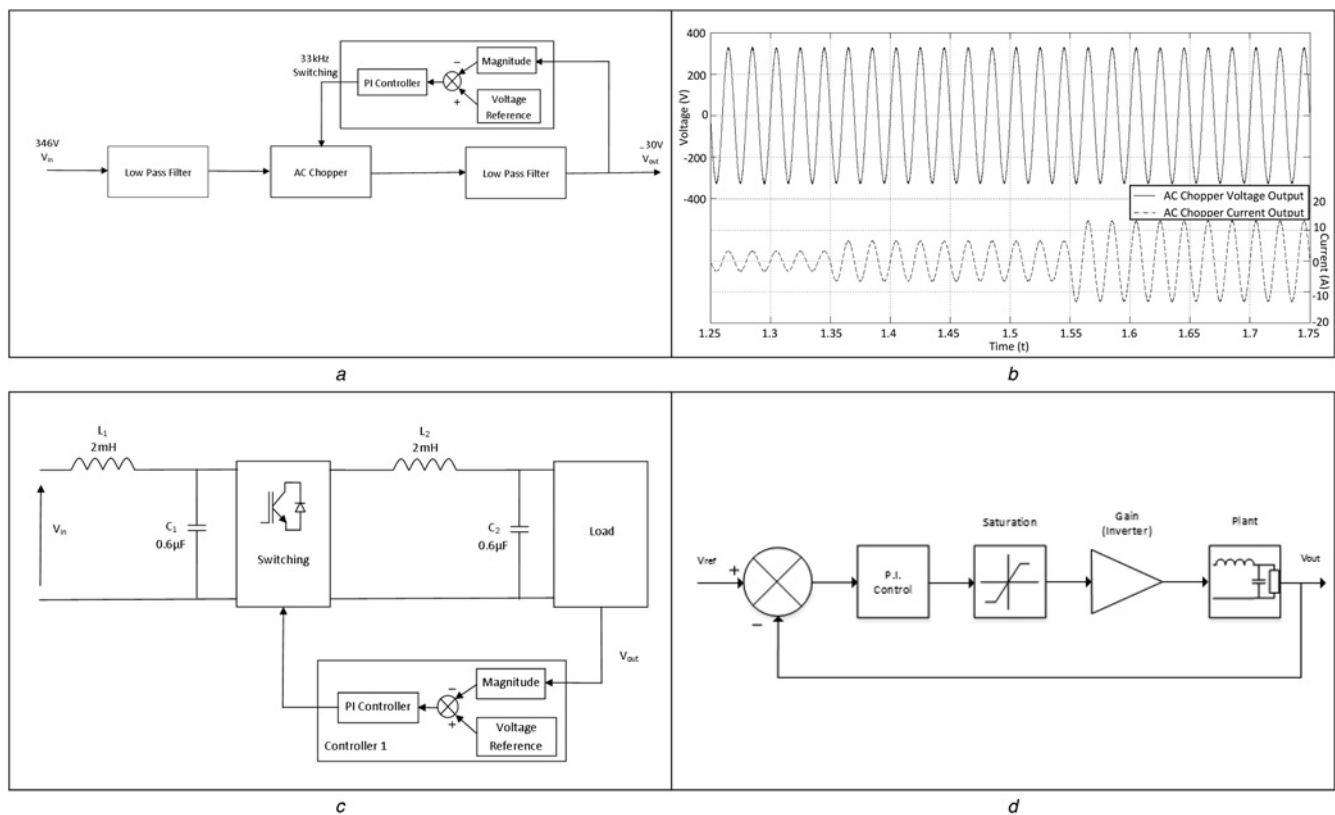
From Figs. 2*d* and 4*a*, it is clear that the AC chopper is much less complex. Table 7 provides a cost estimate comparison of the two solutions based on the principal components in both converter topologies. The costs are based on the power semi-conductors used in Section 4.1 and include values for the power filters [40–42].

From the results, in Table 7 it is clear that the cost of using the back-to-back converter topology to outfit the physical system demonstrated in Section 2.1 is more expensive than outfitting the system with the AC chopper topology. Looking at Section 2.5, the cost reduction in using the AC chopper over the back-to-back inverter will make PUVR more viable in terms of cost benefit.

4.4 Control

4.4.1 Development of closed-loop control for the AC chopper: In order to improve dynamic performance, a closed voltage feedback control loop was placed around the AC chopper. Fig. 5*a* shows the block diagram for this control. The response of the closed-loop control was tested by applying a load step to the output of the chopper. Fig. 5*b* shows that when the load is doubled from 0.5 to 1 kW after 1.35 s the chopper output voltage remains at 230 V and the current doubles from 2.1 to 4.2 A. After 1.55 s the load is further doubled to 2 kW. The output chopper voltage remains at 230 V AC and the current rises to 9 A. In response to the load steps, the output voltage was observed to dip slightly by 1.3 and 1.7 V over 0.03 s for the first and second load steps, respectively, which as a percentage of load is a dip of -0.4 and -0.5% . These dips are caused by the change in load which increases current demand. This results in a voltage dip because of the relationship between voltage and current. The PI controller then adjusts the PWM of the switches to match the demand. The dips are within the British standards for voltage sag, which is $230\text{ V} + 10\text{--}6\%$ [7].

A block diagram for the AC chopper is shown in Fig. 5*c*, with values taken from the filter design section. The closed-loop transfer function was found to be cubic, shown in (10). Fig. 5*d* is a control diagram of the closed loop, the reference is compared with the output then passed to the PI control. The new output of the inverter is then passed through the plant and the cycle continues. In order to tune

**Fig. 5** Closed voltage feedback control loop was placed around the AC chopper

- a* Block diagram of improved chopper with control
b Output voltage and current of the AC chopper
c Block diagram of AC chopper
d Control of the AC chopper

the third-order equation the good gain method was used [43]. Using this method to find approximate values then manual tuning, the ideal values for K_p and K_i were found. See Appendix 3 for all calculated values of controller gain

$$\frac{V_{out}}{V_{in}} = \frac{(K_p/L_2C_2)s + (K_i/L_2C_2)}{s^3 + (1/R_{load}C_2)s^2 + ((K_p + 1)/L_2C_2)s + (K_i/L_2C_2)} \quad (10)$$

4.4.2 Closed-loop back-to-back inverter: A block diagram for the back-to-back inverter is shown in Fig. 6a. In order for the back-to-back inverter to be able to operate correctly V_{out} must not vary with load. To solve this, a feedback loop was placed in the system which measures the V_{out} , compares with a set point of 230 V AC and passes this difference to a PI controller. This controls the switching of the house side inverter (HSI) semiconductors (Fig. 4b) and changes the modulation index of the H bridge dependant on what is required.

The closed-loop HSI was tested using the same means as the AC chopper, demand changes from 0.5 to 1 to 2 kW. The results are shown in Fig. 6b. It is observed that the back-to-back inverter can supply the load with a steady 230 V AC at the different loads. In response to the load steps, the output voltage was observed to dip slightly by 1.9 and 2.1 V over 0.03 s for the first and second load steps, respectively, which as a percentage of load is a dip of -0.6 and -0.65%, this is within the British standards for voltage sag, which is 230 V + 10–6% [7]. Both topologies

perform well within industry standards. See Section 4.2 for more information on power quality.

It can be observed that the inversion stage of the back-to-back inverter in Fig. 6b is identical to the output of the AC chopper in Fig. 5c but with different values of L_2 and C_2 . Therefore Fig. 5d and (10) can be used to describe the control of the inversion stage.

It is worth noting that the initial rectification stage can only ‘boost’ the V_{dc} , therefore the voltage is not able to go below the peak V_{in} of 490 V. This means the modulation index of the inverter stage will be low and this will lead to more loss in the switching of the HSI [44].

In order to control the power flow into the back-to-back inverter from the distribution grid, an additional control loop is required at the grid side rectifier (GSR) as shown as controller 2 in Fig. 6c.

The power flow from the grid to the back-to-back inverter is controlled via two, classic cascaded control loops, where the outer control loop regulates the DC-link voltage and the inner loop regulates the current flowing from the grid through the rectifier. In order to tune controller 2, the speed of the inner and outer loop PI controllers were set to be an order of magnitude apart. This allowed the two control loops to be decoupled and hence operate independently of each other [45, 46]. Therefore the outer control loop was treated as a standard second-order control loop as described in (5) in Section 3.2.3.

Using Fig. 6d, (11) which describes the outer loop and (12) which describes the inner loop (where R is a small line resistance of 1 mΩ) the controller gain vales were calculated. Appendix 3 catalogues the calculated values of controller gain. It was found that these calculated values

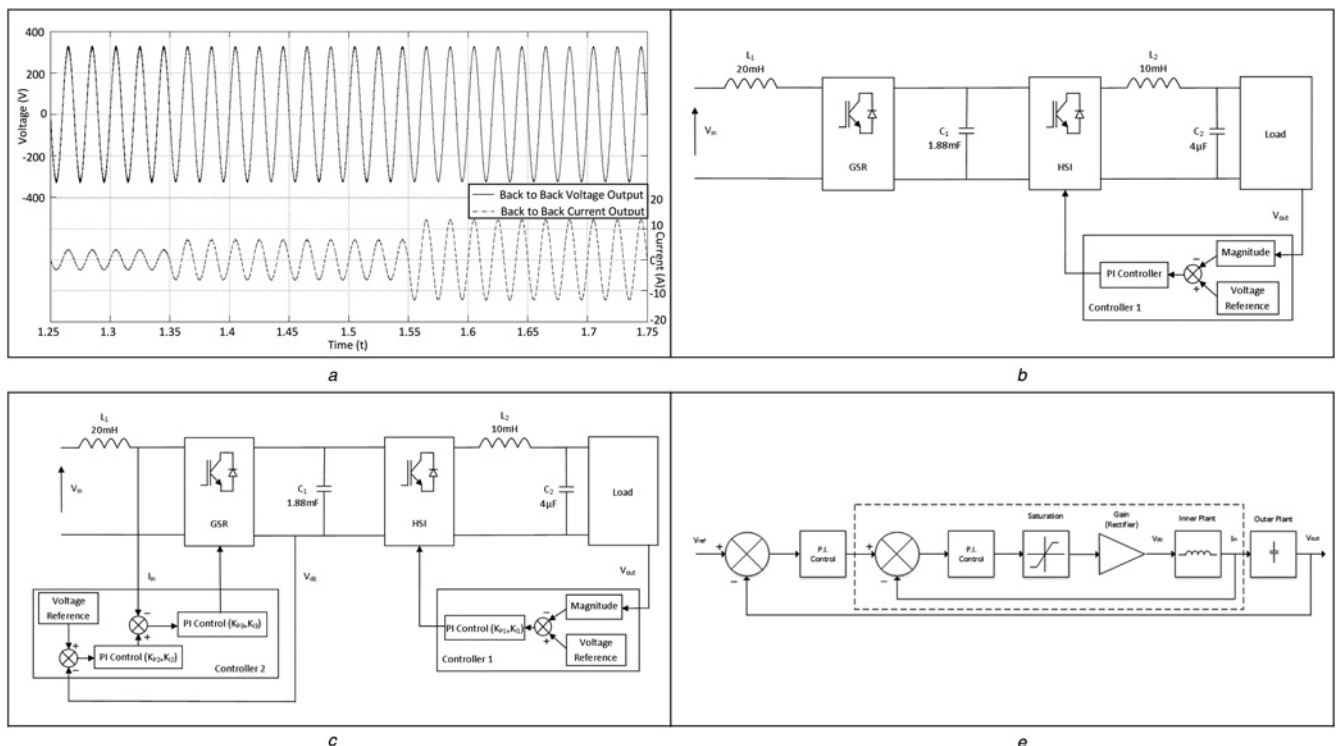


Fig. 6 Block diagram for the back-to-back inverter

- a Output of the back-to-back inverter
- b Block diagram of the back-to-back inverter
- c Back-to-back inverter with second controller
- d Control of the back-to-back inverter rectifier

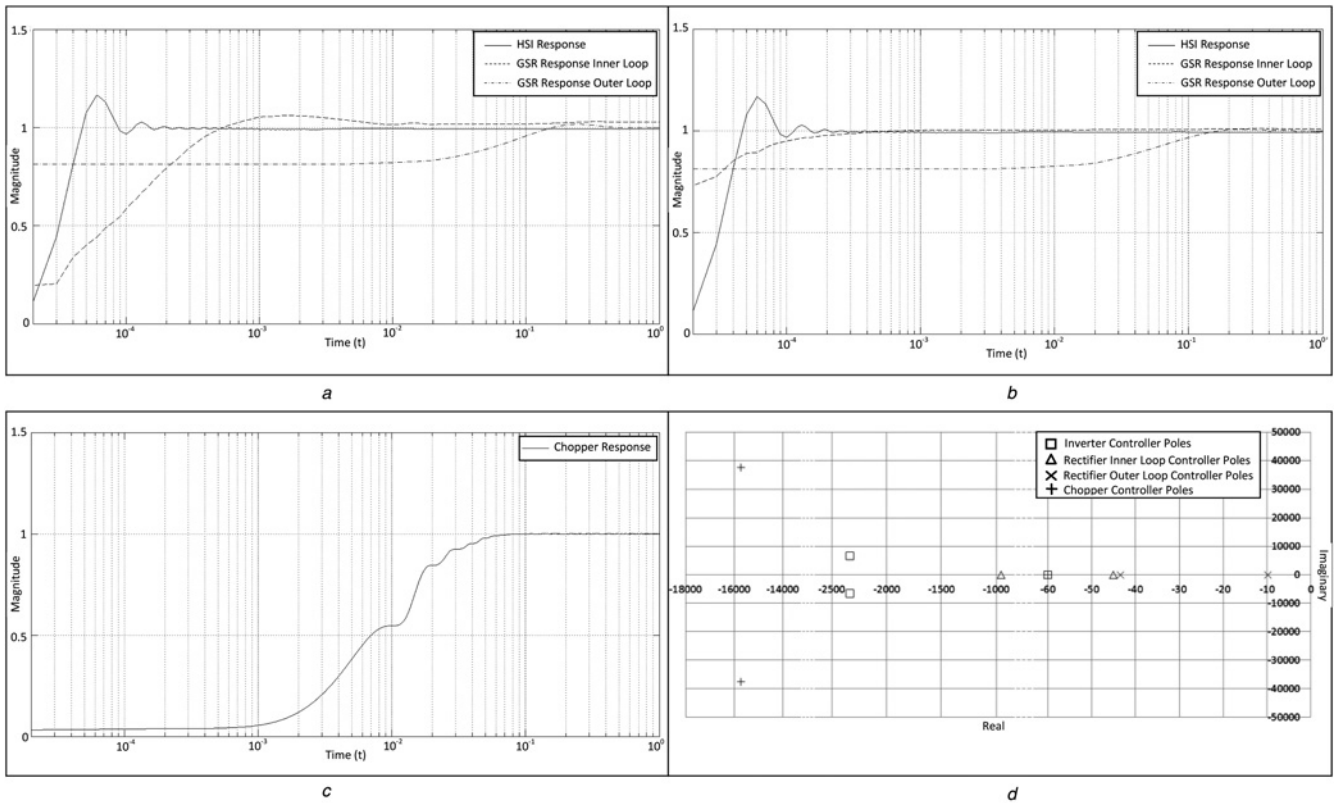


Fig. 7 GSR controllers were manually tuned by increasing
a Step response of back-to-back inverter, with calculated values
b Step response of back-to-back inverter, with subsequently tuned values
c Step response of AC chopper, with tuned values
d Root locus of all controllers

had an overshoot response despite being tuned for over-damping ($\xi = 1$), this is because of the ignored differential term in the numerator of (11) and (12). Therefore the GSR controllers were manually tuned by increasing K_{p2} and K_{p3} , the result of this is shown in Fig. 7*b*. The final control values are catalogued in Appendix 4.

The step response for (10)–(12) is shown in Fig. 7*b*. This demonstrates the speed of the controllers to be sufficiently different, to allow them to be considered decoupled from each other.

The response of the AC chopper is shown in Fig. 7*c*. In order to demonstrate the stability of the controllers the poles of the control loops were plotted in Fig. 7*d*

$$\frac{V_{out}}{V_{in}} = \frac{(K_{i2}/C_1)}{s^2 + (K_{p2}/C_1)s + (K_{i2}/C_1)} \quad (11)$$

$$\frac{V_{out}}{V_{in}} = \frac{(K_{i3}/L_1)}{s^2 + ((R + K_{p3})/L_1)s + (K_{i3}/L_1)} \quad (12)$$

4.5 Transient behaviour

The time taken to reach steady state was found to be 0.1 s for the back-to-back inverter compared to 0.05 s for the AC chopper shown in Figs. 7*b* and *c*. Both topologies are sufficiently fast.

4.6 Protection

The proposed converter location is shown in Fig. 8. To ensure that the breaker on the main feeder does not activate in case of a fault on the converter hardware, the converter must be placed after the fuses on the distribution network. This will prevent a fault in any single converter causing a trip on an entire street.

However, this means that any present protection system must be rated higher than 346 V phase, otherwise it must be replaced. This will not be problematic as British Standards fuses have a voltage rating of up to 1 kV line AC [47].

A standard three bedroom home will have a series of fuses with upstream reclose devices on the main feeder or breakers on the local transformer [48]. Use of either converter increases the fault level substantially, consider a short circuit across the load of 0.1 Ω and (13) [49]

$$P_f = \frac{V_{rms}^2}{R_f} \quad (13)$$

With the present system where $V_{rms} = 230$ V the resulting fault level, P_f , is equal to 0.53 MW. With $V_{rms} = 346$ V the resulting fault level is 1.2 MW, an increase of 0.7 MW.

Therefore both converter types share this common disadvantage. However, if the installation follows IET wiring standards, which considers low voltage to be under

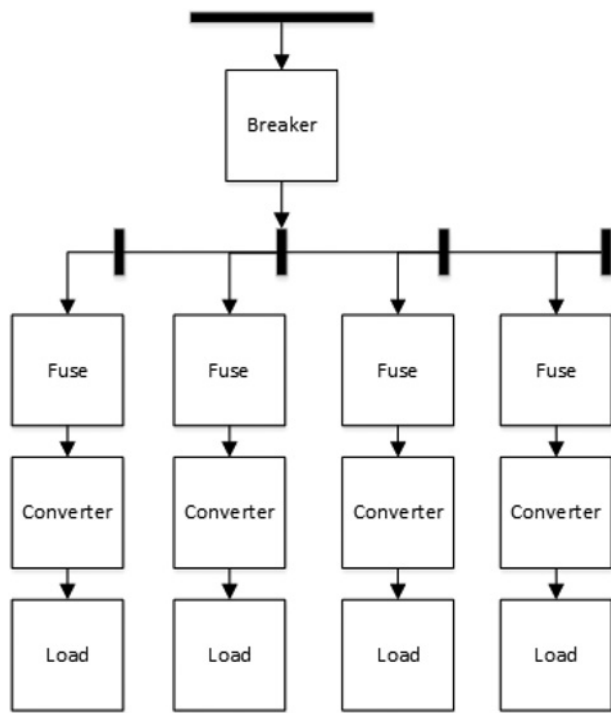


Fig. 8 Proposed converter location

1 kV_{3ph} or 600 V_{ph}, there will be no compromise to safety by increasing the voltage [50].

5 Conclusions

PUVR has been presented as a viable approach to increasing the capacity of urban distribution networks in the UK grid. Of the two possible system architectures considered, it is clear that an AC chopper architecture has several advantages over a back-to-back inverter system. The AC chopper was found to generate less loss, cost less to build, require smaller filters and have simple control.

The back-to-back inverter was found to be better in maintaining power quality seen by both the grid and consumer. The AC chopper is not decoupled from the grid, there is no intermediary buffer, and power quality suffers as a result. Further research would be required to modify the AC chopper in order to make it comparable to the back-to-back inverter in terms of power quality. In addition, if PUVR is implemented, household protection would need to be modified. Miniature circuit breakers and fuses presently operate for a specified amount of current, if the amount of current the end-user can access is increased it follows that household protection systems will need to account for this increase. Further research would be required to modify the AC chopper in order to integrate a protection system.

6 Acknowledgments

The authors acknowledge the funding support of the Engineering and Physical Sciences Research Council (EPSRC), the Power Networks Research Academy (PNRA) and Western Power Distribution for providing utility information.

7 References

- Parsons Brinckerhoff: 'Powering the future' (Parsons Brinckerhoff, 2009)
- Akmal, M., Fox, B., Morrow, D.J., Littler, T.: 'Impact of high penetration of heat pumps on low voltage distribution networks'. IEEE Power Tech, Trondheim, 2011
- 'Cost of Fuel': <http://www.whatgas.com/petrol-prices/fuel-cost.html#UiCYRusim4>, accessed November 2012
- National Grid: 'UK future energy scenarios' (National Grid, 2011)
- BS5467: 'Electric cables. Thermosetting insulated, armoured cables for voltages of 600 V/1000 V and 1900/3300 V', 1997
- Meier, A.V.: 'The physics of electricity', in Desurvire, E. (Ed.): 'Electric power systems: a conceptual introduction' (John Wiley and Sons, 2006), pp. 8–13
- 'Electrical Supply Tolerances and Electrical Appliance Safety': <http://www.bis.gov.uk/files/file11548.pdf>, accessed November 2012
- Thomson, M., Infield, D.G.: 'Impact of widespread photovoltaics generation on distribution systems', *IET Renew. Power Gener.*, 2007, 1, (1), pp. 33–40
- Liu, Y., Bebic, J., Kroposki, B., de Bedout, J., Ren, W.: 'Distribution system voltage performance analysis for high-penetration PV'. IEEE Energy 2030 Conf., Atlanta, Georgia, November 2008
- Cipcigan, L.M., Taylor, P.C.: 'Investigation of the reverse power flow requirements of high penetrations of small-scale embedded generation', *IET Renew. Power Gener.*, 2007, 1, (3), pp. 160–166
- Qian, H., Lai, J.-S., Zhang, J., Yu, W.: 'High-efficiency bidirectional AC-DC converter for energy storage systems', IEEE Energy Conversion Congress and Exposition (ECCE), Atlanta, Georgia, September 2010
- El Hayek, J.: 'Transformer design as a key for efficiency optimization'. XIX Int. Conf. on Electrical Machines (ICEM), Rome, Italy, September 2010
- 'Siemens SINAMICS G110 3.0 kW 1-phase Frequency Inverter', <http://www.conrad-electronic.co.uk/ce/en/product/198185/Siemens-SINAMICS-G110-30-kW-1-phase-frequency-inverter-230-VAC-to-6SL3211-0AB23-0AA1/1101123>, accessed November 2012
- 'SQUARE D | Transformer 3kva': <http://www.easupplies.com/SQUARE-D-3S4F-Transformer-3K-Watt-1-Phase-600V-P-p/el516e.htm>, accessed November 2012
- 'Commercial Transformers': http://www.voltageconverters.com/commercial_transformers.html, accessed May 2010
- 'Power Electronic Inverters': <http://www.dhgate.com/wholesale/store/f808081365d19ec013670c9d7db2496.html>, accessed May 2013
- Hill, G., Blythe, P.T., Hubner, Y., Neaimeh, M., Higgins, C., Suresh, V.: 'Monitoring and predicting charging behaviour for electric vehicles'. IEEE Intelligent Vehicles Symp. (IV), Madrid, Spain, June 2012
- Yilmaz, M., Krein, P.T.: 'Review of the impact of vehicle-to-grid technologies on distribution systems and utility interfaces', *IEEE Power Electronics*, 2013, 28, (12), pp. 5673–5689
- Söderberg, D., Engdahl, H.: 'Using 1 kV low voltage distribution for connection of plug-in vehicles'. IEEE PES Innovative Smart Grid Technologies Conf. Europe (ISGT Europe), Gothenburg, Sweden, October 2010
- Harris, A.: 'Charge of the electric car', *Eng. Technol.*, 2009, 4, (10), pp. 52–53
- 'Metered Half-Hourly Electricity Demands': <http://www.nationalgrid.com/uk/Electricity/Data/Demand+Data/>, accessed November 2012
- Berry, R.U.: 'Possibilities of heat pumps for heating homes', *Am. Inst. Electr. Eng.*, 1944, 63, (9), pp. 619–622
- Baird, P.J., Herman, H., Stevens, G.C.: 'Rapid non-destructive condition assessment of insulating materials'. IEEE Int. Symp. on Electrical Insulation (ISEI), Vancouver, Canada, June 2008
- 'Inverter Home - APV 1700-2M-TL | RADIUS': <http://www.radius-gefran.co.uk/products/home-inverters/apv-1700-2m-tl>, accessed November 2012
- Kolar, J.W., Baumann, M., Schafmeister, F., Ertl, H.: 'Novel three-phase AC-DC-AC sparse matrix converter'. IEEE Applied Power Electronics Conf. (APEC), Dallas, Texas, March 2002
- Mohan, N., Undeland, T.M., Robbins, W.P.: 'Optimising the utility interface with power electronics', 'Bipolar junction transistors', in Zobrist, B. (Ed.): 'Power electronics: converters, applications, and design' (John Wiley & Sons, 2002, 3rd edn.), pp. 490–565
- Scottish and Southern Energy: 'Statement of methodology and charges for connection to Scottish hydro electric power distribution plc's electricity distribution system' (Scottish and Southern Energy, 2013), pp. 130–140
- 'Solar Inverters': <http://www.pvsupplies.co.uk/5-grid-tie-inverters>, accessed August 2013

- 29 'Commander SK SK4402 37 kW (45 kW) Inverter, 3-phase 480 V Input, 3-phase 480 V Output': http://www.motorcontrolwarehouse.co.uk/commander-sk-sk4402/prod_289.html, accessed August 2013
- 30 Jorgenson, D.W., Wessner, C.W.: 'Moore's law and the economics of semiconductor price trends', in Jorgenson, D.W., Wessner, C.W. (Eds.): 'Productivity and cyclicalities in semiconductors: trends, implications, and questions – report of a symposium', (The National Academies Press, 2004), pp. 151–170
- 31 Dugan, R.C., Mcgranaghan, M.F.F., Santoso, S., Beaty, H.W.: 'Terms and definitions', and 'distributed generation and power quality', in: 'Electrical Power Systems Quality' (McGraw-Hill, 2012, 3rd edn.), pp. 12–43, 417–418
- 32 IEEE 1491: 'Battery Monitoring', 2005
- 33 Malesani, L., Rossetto, L., Tenti, P., Tomasin, P.: 'AC/DC/AC PWM converter with reduced energy storage in the DC-link'. IEEE Industry Applications, Orlando, Florida, October 1995, pp. 287–292
- 34 'Calculating Voltage Ripple': http://www.tonic-lab.com/pdf/reading_room/electronics_Vrip.pdf, accessed May 2013
- 35 'Insulated Gate Bipolar Transistor with Ultrafast Soft Recovery Diode': <http://www.farnell.com/datasheets/34696.pdf>, accessed February 2004
- 36 '75A, 1200 V Hyperfast Diode': <http://www.farnell.com/datasheets/1729228.pdf>, accessed April 2013
- 37 Wang, B., Venkataramanan, G.: 'Analytical modeling of semiconductor losses in matrix converters'. IEEE Int. Power Electronics and Motion Control Conf. (IPEMC), Shanghai, China, August 2006
- 38 Casanellas, F.: 'Losses in PWM Inverters using IGBTs', *IEE Proc., Electr. Power Appl.*, 1994, **141**, (5), pp. 235–239
- 39 Jianhong, C., Lie, T.T., Vilathgamuwa, D.M.: 'Basic control of interline power flow controller'. IEEE Power Engineering Society Winter Meeting, New York City, New York, January 2002
- 40 'ARW Transformers': <http://www.arwtransformers.co.uk/default.htm>, accessed October 2013
- 41 'Kemet – C322C473KCR5CA – Capacitor, 47nF, 500 V, X7R': <http://www.uk.farnell.com/kemet/c322c473kcr5ca/capacitor-47nf-500v-x7r/dp/1288233?Ntt=1288233>, accessed October 2013
- 42 'BHC Components – ALS30A222NP500 – Capacitor, 2200UF, 500 V, 2013': <http://www.uk.farnell.com/bhc-components/als30a222np500/capacitor-2200uf-500v/dp/536519?Ntt=536519>, accessed October 2013
- 43 Haugen, F.: 'The good gain method for simple experimental tuning of PI controllers', *Model. Identif. Control*, 2012, **33**, (4), pp. 141–152
- 44 Srinivasan, R., Oruganti, R.: 'A unity power factor converter using half-bridge boost topology'. *IEEE Trans. Power Electron.*, 1998, **13**, (3), pp. 487–500
- 45 'Tuning Cascade Loops': <http://www.controlglobal.com/articles/2005/547.html>, accessed April 2013
- 46 Minxia, Z., Atherton, D.P.: 'Optimum cascade PID controller design for SISO systems'. Int. Conf. on Control, Coventry, UK, March 1994
- 47 'BS88 Fuses': <http://www.fuses.bs88.eu/>, accessed November 2012
- 48 Emhemed, A.S., Burt, G., Anaya-Lara, O.: 'Impact of high penetration of single-phase distributed energy resources on the protection of LV distribution networks'. Universities Power Engineering Conf. (UPEC), Brighton, UK, September 2007
- 49 Glover, J.D., Sarma, M.S., Overbye, T.J.: 'Fundamentals', in Gowans, H. (Ed.): 'Power System Analysis and Design' (Cengage Learning, 2010, 4th edn.), pp. 44–50
- 50 I.E.E.: 'Scope, object and fundamental requirements for safety', in: 'Regulations for Electrical Installations' (I.E.E., 1987, 15th edn.), p. 2

8 Appendix

8.1 Appendix 1

See Table 8.

8.2 Appendix 2

See Table 9.

8.3 Appendix 3

See Table 10.

8.4 Appendix 4

See Table 11.

Table 8 Power world cable data

Cable	Cable resistance, Ω	Cable reactance, $\mu\Omega$	Cable thermal limit, MVA
1	0.006992	0.0031188	0.34431
2	0.00564	0.0021	0.22287
3	0.00188	0.0007	0.22287
4	0.00188	0.0007	0.22287
5	0.012	0.00555	0.22287
6	0.01128	0.0042	0.22287
7	0.049555	0.00646	0.12282
8	0.01222	0.00455	0.22287
9	0.01222	0.00455	0.22287
10	0.00583	0.00076	0.12282
11	0.014575	0.0019	0.12282
12	0.014575	0.0019	0.12282
13	0.0112	0.00518	0.26841
14	0.0188	0.007	0.22287
15	0.0016	0.00074	0.26841
16	0.0016	0.00074	0.26841
17	0.0216	0.00999	0.26841
18	0.0128	0.00592	0.26841
19	0.0192	0.00441	0.18354
20	0.0064	0.00147	0.18354
21	0.00583	0.00076	0.12282
22	0.00752	0.0028	0.22287
23	0.008745	0.00114	0.12282
24	0.008745	0.00114	0.12282
25	0.000376	0.00014	0.22287
26	0.02256	0.0084	0.22287
27	0.024	0.0055125	0.18354
28	0.00846	0.00315	0.22287
29	0.00752	0.0028	0.22287
30	0.016	0.0074	0.26841
31	0.0008	0.00037	0.26841
32	0.00188	0.0007	0.22287
33	0.0216	0.00999	0.26841
34	0.0094	0.0035	0.22287
35	0.00583	0.00076	0.12282
36	0.0047	0.00175	0.22287
37	0.00583	0.00076	0.12282
38	0.01166	0.00152	0.12282
39	0.008745	0.00114	0.12282

Table 9 Non-linear power draw data from devices

	DC power draw	
	Voltage, V	Current, A
laptop	19	4.74
TV	66.7	1.5
games console	12	3.7
PC	12	17
monitor	66.7	1.5

Table 10 Calculated values of controller gain

	K_{p1}	K_{i1}	K_{p2}	K_{i2}	K_{p3}	K_{i3}
AC chopper	1	120	—	—	—	—
back-to-back inverter	1	120	0.077	0.8	0.85	860

Table 11 Final manually tuned values of controller gain

	K_{p1}	K_{i1}	K_{p2}	K_{i2}	K_{p3}	K_{i3}
AC chopper	1	120	—	—	—	—
back-to-back inverter	1	120	0.1	0.8	50	860